

## Cytokine Binding by Polysaccharide–Antibody Conjugates

Liang Tso Sun,<sup>†</sup> Kyle S. Buchholz,<sup>†</sup> Michael T. Lotze,<sup>‡,§,||</sup> and Newell R. Washburn<sup>\*,†,||,⊥</sup>

Departments of Biomedical Engineering and Chemistry, Carnegie Mellon University, Pittsburgh, Pennsylvania 15213, and Departments of Surgery and Bioengineering and McGowan Institute for Regenerative Medicine, University of Pittsburgh, Pittsburgh, Pennsylvania 15213

Received May 4, 2010; Revised Manuscript Received July 22, 2010; Accepted August 20, 2010

**Abstract:** Cytokine-neutralizing antibodies are used in treating a broad range of inflammatory conditions. We demonstrate that monoclonal antibodies against interleukin-1 $\beta$  and tumor necrosis factor- $\alpha$  were still active when conjugated to high molecular weight polysaccharides. These polysaccharides are hydrophilic, but their size makes them unable to circulate in the bloodstream when delivered to tissues, opening up the possibility of localized treatment of inflammatory conditions. To explore this new class of protein–polysaccharide conjugates, we covalently modified interleukin-1 $\beta$  and tumor necrosis factor- $\alpha$  monoclonal antibodies with high molecular weight hyaluronic acid and carboxymethylcellulose. Rigorous purification using dialysis with a 300 kDa-cutoff membrane removed unconjugated monoclonal antibodies. We characterized the composition of the constructs and demonstrated using molecular binding affinity measurements and cell assays that the conjugates were capable of binding proinflammatory cytokines. The binding affinities of both the unconjugated antibodies for their cytokines were measured to be approximately 120 pM. While all conjugates had pM-level binding constants, they ranged from 40 pM for the hyaluronic acid–(anti-interleukin-1 $\beta$ ) conjugate to 412 pM for the carboxymethylcellulose–(anti-interleukin-1 $\beta$ ) conjugate. Interestingly, the dissociation time constants varied more than the association time constants, suggesting that conjugation to a high molecular weight polysaccharide did not interfere with the formation of the antibody–cytokine complex but could stabilize or destabilize it once formed. Conjugation of cytokine-neutralizing antibodies to high molecular weight polymers represents a novel method of delivering anticytokine therapeutics that may avoid many of the complications associated with systemic delivery.

**Keywords:** Antibody; cytokine; inflammation; polysaccharide

## 1. Introduction

Cytokine signaling networks are a critical component in the response to injury and disease,<sup>1</sup> and cytokine-neutralizing antibodies are effective therapeutic strategies in treating a

broad range of inflammatory conditions.<sup>2</sup> However, serious side effects have been reported when these compounds are administered systemically due to their immunosuppressive nature.<sup>3</sup> Strategies need to be developed to avoid the risks that occur with systemic delivery.

Conjugating polymers to therapeutic proteins has been an extensively explored approach to modulate their pharmacokinetics *in vivo* and enhance their efficacy. The synthetic polymer poly(ethylene glycol) (PEG) has been extensively

\* Corresponding author. Mailing address: Department of Chemistry, Carnegie Mellon University, Pittsburgh, PA 15213. Phone: (412)268-2130. Fax: (412)268-6897. E-mail: washburn@andrew.cmu.edu.

<sup>†</sup> Department of Biomedical Engineering, Carnegie Mellon University.

<sup>‡</sup> Department of Surgery, University of Pittsburgh.

<sup>§</sup> Department of Bioengineering, University of Pittsburgh.

<sup>||</sup> McGowan Institute for Regenerative Medicine, University of Pittsburgh.

<sup>⊥</sup> Department of Chemistry, Carnegie Mellon University.

(1) Thomson, A. W.; Lotze, M. T. *The Cytokine Handbook*, 4th ed.; Academic Press: London, 2003; p 1536.

(2) Brekke, O. H.; Sandlie, I. Therapeutic antibodies for human diseases at the dawn of the twenty-first century. *Nat. Rev. Drug Discovery* **2003**, 2 (1), 52–62.

(3) Bongartz, T.; Sutton, A. J.; Sweeting, M. J.; Buchan, I.; Matteson, E. L.; Montori, V. Anti-TNF antibody therapy in rheumatoid arthritis and the risk of serious infections and malignancies: systematic review and meta-analysis of rare harmful effects in randomized controlled trials. *JAMA, J. Am. Med. Assoc.* **2006**, 295 (19), 2275–85.

used to engineer therapeutic molecules because of its biologically inert nature and excellent solubility in aqueous media.<sup>4–6</sup> The primary objective of this type of conjugation is to prolong the circulation time of these molecules by reducing their renal clearance rates. The PEG molecular weights tend to range between 20 and 60 kDa,<sup>7,8</sup> which appears to balance improvements in circulation time with retention of biological activities. These conjugated polymers also protect therapeutic proteins from immune responses and enzymatic attack, thus increasing stability of these therapeutic agents *in vivo*, with the overall goal of increasing the systemic activity of the proteins.<sup>4</sup>

However, the main challenge facing clinical application of cytokine-neutralizing antibodies is not improving circulation time but rather developing delivery strategies to avoid side effects associated with systemic delivery. For example, antibodies against tumor necrosis factor- $\alpha$  (TNF- $\alpha$ ) or interleukin-1 $\beta$  (IL-1 $\beta$ ) or other cytokines have been used to treat rheumatoid arthritis, Crohn's disease, ankylosing spondylitis, psoriasis, and other inflammatory conditions.<sup>9,10</sup> (A PEGylated anti-TNF- $\alpha$  Fab fragment, Cimzia, has received extensive clinical use.<sup>11</sup>) While effective at controlling the inflammatory disorder, patients on anti-TNF- $\alpha$  therapy have increased rates of complications, such as tuberculosis, due to the immunosuppressive effects of the drug.<sup>3</sup> While some therapeutic antibodies, such as the inhibitor of vascular endothelial growth factor Avastin,<sup>12</sup> have been injected locally, there are few reports of direct application of cytokine-neutralizing antibodies to sites of inflammation.<sup>13</sup> Many of the conditions treated with cytokine-neutralizing antibodies,

such as psoriasis,<sup>14</sup> have a significant component of the symptoms that is characterized by local inflammation, and being able to treat the local inflammation locally could avoid many of these systemic side effects. This approach could also make cytokine-neutralizing antibodies applicable to a broad range of dermatological conditions, where topical application of a gel is a standard treatment strategy.<sup>15</sup>

We propose that mAb conjugation to high molecular weight, hydrophilic polymers which are incapable of entering the circulatory system could be a novel strategy for accomplishing this. Several high molecular weight biopolymers could be suitable for this approach, and hyaluronic acid (HA) and carboxymethylcellulose (CMC) were explored in this work. HA is a glycosaminoglycan and a major component of ECM, and recombinant versions, such as that used in this work, can have  $M_w$  of 1.6 MDa. HA has intrinsic biological activities and has been used to promote wound healing. It exhibits unique properties to stimulate cell motility through CD44 and RHAMM receptors,<sup>16,17</sup> and its degradation products can act as damage associated molecular patterns (DAMPs) to modulate the immunological response at the injury site.<sup>18,19</sup> While the half-life of subcutaneously implanted HA has been measured to be about 50 h,<sup>20</sup> it is impossible to predict the half-life of the chemically processed mAb conjugate *in vivo*. It is similarly difficult to predict the full range of immunological effects of cytokine-neutralizing antibodies conjugated to HA, although preliminary *in vivo* studies suggested that subcutaneous delivery of anti-IL-1 $\beta$  and anti-TNF- $\alpha$  conjugated to HA did have a strong anti-

- (4) Veronese, F. M.; Pasut, G. PEGylation, successful approach to drug delivery. *Drug Discovery Today* **2005**, *10* (21), 1451–8.
- (5) Kubetzko, S.; Sarkar, C. A.; Pluckthun, A. Protein PEGylation decreases observed target association rates via a dual blocking mechanism. *Mol. Pharmacol.* **2005**, *68* (5), 1439–1454.
- (6) Molineux, G. Pegylation: engineering improved biopharmaceuticals for oncology. *Pharmacotherapy* **2003**, *23* (8 Part 2), 3S–8S.
- (7) Thomas, T.; Foster, G. Nanomedicines in the treatment of chronic hepatitis C--focus on pegylated interferon alpha-2a. *Int. J. Nanomed.* **2007**, *2* (1), 19–24.
- (8) Zamboni, W. C. Pharmacokinetics of pegfilgrastim. *Pharmacotherapy* **2003**, *23* (8 Part 2), 9S–14S.
- (9) Carter, P. H.; Zhao, Q. Clinically validated approaches to the treatment of autoimmune diseases. *Expert Opin. Invest. Drugs* **2010**, *19* (2), 195–213.
- (10) Rozenblit, M.; Lebowitz, M. New biologics for psoriasis and psoriatic arthritis. *Dermatol. Ther.* **2009**, *22* (1), 56–60.
- (11) Goel, N.; Stephens, S. Certolizumab pegol. *mAbs* **2010**, *2* (2), 137–147.
- (12) Avery, R. L.; Pieramici, D. J.; Rabena, M. D.; Castellarin, A. A.; Nasir, M. A.; Giust, M. J. Intravitreal bevacizumab (Avastin) for neovascular age-related macular degeneration. *Ophthalmology* **2006**, *113* (3), 363372 e5.
- (13) Streit, M.; Belezny, Z.; Braathen, L. R. Topical application of the tumour necrosis factor-alpha antibody infliximab improves healing of chronic wounds. *Int. Wound J.* **2006**, *3* (3), 171–9.

- (14) Ferrandiz, C.; Carrascosa, J. M.; Boada, A. A new era in the management of psoriasis? The biologics: facts and controversies. *Clin. Dermatol.* **2010**, *28* (1), 81–7.
- (15) Robson, M. C.; Steed, D. L.; Franz, M. G. Wound healing: biologic features and approaches to maximize healing trajectories. *Curr. Probl. Surg.* **2001**, *38* (2), 72–140.
- (16) Savani, R. C.; Cao, G.; Pooler, P. M.; Zaman, A.; Zhou, Z.; DeLisser, H. M. Differential involvement of the hyaluronan (HA) receptors CD44 and receptor for HA-mediated motility in endothelial cell function and angiogenesis. *J. Biol. Chem.* **2001**, *276* (39), 36770–8.
- (17) Bourguignon, L. Y.; Gilad, E.; Peyrollier, K.; Brightman, A.; Swanson, R. A. Hyaluronan-CD44 interaction stimulates Rac1 signaling and PKN gamma kinase activation leading to cytoskeleton function and cell migration in astrocytes. *J. Neurochem.* **2007**, *101* (4), 1002–17.
- (18) Termeer, C.; Benedix, F.; Sleeman, J.; Fieber, C.; Voith, U.; Ahrens, T.; Miyake, K.; Freudenberg, M.; Galanos, C.; Simon, J. C. Oligosaccharides of Hyaluronan activate dendritic cells via toll-like receptor 4. *J. Exp. Med.* **2002**, *195* (1), 99–111.
- (19) Tesar, B. M.; Jiang, D.; Liang, J.; Palmer, S. M.; Noble, P. W.; Goldstein, D. R. The role of hyaluronan degradation products as innate alloimmune agonists. *Am. J. Transplant.* **2006**, *6* (11), 2622–35.
- (20) Laurent, U. B.; Fraser, J. R.; Laurent, T. C. An experimental technique to study the turnover of concentrated hyaluronan in the anterior chamber of the rabbit. *Exp. Eye Res.* **1988**, *46* (1), 49–58.

inflammatory effect.<sup>21</sup> Although the complex immunological effects of HA are not entirely understood,<sup>22</sup> there may be wound-healing applications of HA–mAb conjugates for which simultaneous activation of CD44/RHAMM and suppression of cytokine-signaling networks is beneficial.<sup>23</sup> As the HA degrades, its actions as a DAMP would be exerted upon an inflammatory microenvironment that could be significantly attenuated, potentially recruiting leukocytes but shifting their actions toward a reparative phenotype. While highly speculative at this point, combinations of biologically potent polysaccharides and antibodies open up possibilities for new approaches to therapeutics development.

Carboxymethylcellulose (CMC) is a derivative of cellulose, which has been extensively functionalized with carboxylic acid groups through chemical processing. In the CMC used in these experiments, the polymer was primarily linear with a reported  $M_w$  of 700 kDa, and the ratio of carboxylic acid groups to CMC monomers was 0.9. The biological activity of cellulose has also been extensively explored, and the implantation of CMC showed no signs of material-induced inflammation or host rejection, indicating that CMC is biocompatible and immunologically inert. CMC also has other attractive properties for conjugating therapeutics, providing ease of modification and delivery in aqueous media. High molecular weight CMC (defined here as greater than 100 kDa) has a much longer persistence time than HA when implanted.<sup>24</sup> So in addition to its lack of biological activity compared to HA, it also provides a method for sustained delivery.

Direct delivery of unconjugated antibodies to sites of inflammation runs the risk of systemic delivery via broken or immature blood vessels or where the dermis is compromised.<sup>25</sup> Indeed, despite the drag forces that tissues exert on diffusing mAb, therapeutic mAb have been shown to readily permeate tissues.<sup>26</sup> The diffusion constant of mAb in buffer solution has been measured to be  $6.3 \times 10^{-7} \text{ cm}^2/\text{s}$  (assuming a hydrodynamic radius of 52 Å) while, in tissues,

the diffusion constant is of order  $10^{-8}$ – $10^{-9} \text{ cm}^2/\text{s}$ .<sup>27</sup> Conjugation of mAb to high molecular weight polysaccharides could localize their activities. With molecular weights greater than 100 kDa, even water-soluble polymers have extensive interactions with surrounding tissues (based on energetic estimates of  $\sim 5 k_B T$  per hydrogen bond<sup>28</sup>) that hinder diffusion in tissue. The self-diffusion constant of 1.5 MDa hyaluronic acid (HA) in aqueous solution has been measured to be  $3.0 \times 10^{-8} \text{ cm}^2/\text{s}$ ,<sup>29</sup> but in tissues this is known to decrease by at least 2 orders of magnitude, suggesting that HA transport in tissues is quite slow.<sup>30</sup> If localizing delivery in tissues is determined largely by diffusion, then conjugation to high molecular weight biopolymers will increase mAb residence time by a factor of at least 10.

In a previous study, we conjugated antitumor necrosis factor- $\alpha$  (anti-TNF- $\alpha$ ) and anti-interleukin- $1\beta$  (anti-IL- $1\beta$ ) monoclonal antibodies to high molecular weight HA and demonstrated the neutralizing activities of these cytokines both *in vitro* and *in vivo*.<sup>21</sup> Significant reductions in the numbers of invading macrophages and shifts in their phenotypes in a rat incisional wound model were observed following treatment with 100  $\mu\text{g}$ , compared to standard systemic doses in humans of 3 mg/kg.<sup>14</sup> This approach has the potential for increased antibody activities at significantly lower doses and the potential for locally controlling inflammation.

In this study, we prepared polysaccharide–mAb constructs using HA and CMC conjugated to anti-IL- $1\beta$  or anti-TNF- $\alpha$  separately and compared their binding and neutralization capabilities to unconjugated mAb. We performed both molecular binding affinity measurements and cellular assays of cytokine activities to understand polysaccharide–mAb interactions in this novel approach to delivering mAb.

## 2. Materials and Methods

**2.1. Materials.** Hyaluronic acid (HA,  $M_w \sim 1.6 \text{ MDa}$ ), carboxymethyl cellulose (CMC,  $M_w \sim 700 \text{ kDa}$ ) with 90% carboxylation per CMC monomer (provided by manufacturer), glycidyl methacrylate, *N*-hydroxysulfosuccinimide sodium salt (sulfo-NHS), *N*-(3-dimethylaminopropyl)-*N'*-ethylcarbodiimide hydrochloride (EDC), and 4-(dimethylamino)pyridine (4-DMAP) were purchased from Sigma-Aldrich (St. Louis, MO) and used as received. Anti-IL- $1\beta$  and anti-TNF- $\alpha$ , both from purified mouse monoclonal IgG1 against human cytokines, were purchased from R&D Sys-

- (21) Sun, L. T.; Bencherif, S. A.; Farkas, A. M.; Gilbert, T. W.; Lotze, M. T.; Washburn, N. R. Biological activities of cytokine-neutralizing antibody-polymer conjugates. *Wound Repair Regen.* **2010**, *18* (3), 302–310.
- (22) Jiang, D.; Liang, J.; Noble, P. W. Hyaluronan in tissue injury and repair. *Annu. Rev. Cell Dev. Biol.* **2007**, *23*, 435–61.
- (23) Steed, D. L.; Ricotta, J. J.; Prendergast, J. J.; Kaplan, R. J.; Webster, M. W.; McGill, J. B.; Schwartz, S. L. Promotion and acceleration of diabetic ulcer healing by arginine-glycine-aspartic acid (RGD) peptide matrix. RGD Study Group. *Diabetes Care* **1995**, *18* (1), 39–46.
- (24) Falcone, S. J.; Doerfler, A. M.; Berg, R. A. Novel synthetic dermal fillers based on sodium carboxymethylcellulose: comparison with crosslinked hyaluronic acid-based dermal fillers. *Dermatol. Surg.* **2007**, *33*, S136–43, discussion S143.
- (25) Karande, P.; Mitragotri, S. Enhancement of transdermal drug delivery via synergistic action of chemicals. *Biochim. Biophys. Acta* **2009**, *1788* (11), 2362–73.
- (26) van Osdol, W.; Fujimori, K.; Weinstein, J. N. An analysis of monoclonal antibody distribution in microscopic tumor nodules: consequences of a binding site barrier. *Cancer Res.* **1991**, *51* (18), 4776–84.

- (27) Clauss, M. A.; Jain, R. K. Interstitial transport of rabbit and sheep antibodies in normal and neoplastic tissues. *Cancer Res.* **1990**, *50* (12), 3487–92.
- (28) Israelachvili, J. *Intermolecular & Surface Forces*, 2nd ed.; Academic Press: London, 1992; p 450.
- (29) Kaminski, T.; Siebrasse, J. P.; Gieselmann, V.; Kubitscheck, U.; Kappler, J. Imaging and tracking of single hyaluronan molecules diffusing in solution. *Glycoconjugate J.* **2008**, *25* (6), 555–60.
- (30) Klein, J.; Meyer, F. A. Tissue structure and macromolecular diffusion in umbilical cord. Immobilization of endogenous hyaluronic acid. *Biochim. Biophys. Acta* **1983**, *755* (3), 400–11.



tems, Inc. (Minneapolis, MN) with reported binding affinities for their cytokines of 120 pM. Recombinant human IL-1 $\beta$  (IL-1F2) and human TNF- $\alpha$  were also purchased from R&D Systems, Inc. All reagents were reconstituted and stored according to the manufacturer's instructions.

**2.2. HA-mAb and CMC-mAb Preparation.** The first step of the reaction consisted of activation of the HA or CMC carboxylic acid groups. The NHS active ester is a versatile precursor for bioconjugation via primary amines,<sup>31,32</sup> although questions still remain regarding its mechanism.<sup>33</sup> The HA-active ester and CMC-active ester intermediates were subsequently used as precursors for the coupling reaction with anti-IL-1 $\beta$  mAb or anti-TNF- $\alpha$  mAb. HA (12 mg, 7.5 nmol) was dissolved in 1 mL of phosphate buffer saline (pH  $\sim$ 7.4). EDC (240  $\mu$ g, 1.55  $\mu$ mol), sulfo-NHS (650  $\mu$ g, 3.00  $\mu$ mol), and 4-DMAP (10  $\mu$ g) were added as solids to the HA solution and allowed to dissolve and react overnight before adding mAb. Either anti-IL-1 $\beta$  mAb or anti-TNF- $\alpha$  mAb (1.0 mg, 6.66 nmol) was dissolved in 200  $\mu$ L of PBS and then added to the activated HA solution. The reaction proceeded at 4  $^{\circ}$ C overnight. The solution was then twice precipitated in a saturated solution of ammonium sulfate, and the product was recovered by centrifugation. The pellet was reconstituted in PBS and followed by dialysis using Fast Spin Dialyzer and MWCO 300 kDa cellulose membrane (Nest Group, Southborough, MA) against pure PBS overnight with four changes of solutions.

CMC (12 mg, 17.1 nmol) was dissolved in 1 mL of phosphate buffer saline (pH  $\sim$ 7.4). EDC (240  $\mu$ g, 1.55  $\mu$ mol), sulfo-NHS (650  $\mu$ g, 3.00  $\mu$ mol), and 4-DMAP (10  $\mu$ g) were added as solids to the HA solution and allowed to dissolve and react overnight before adding mAb. Anti-IL-1 $\beta$  mAb and anti-TNF- $\alpha$  mAb (0.5 mg, 3.33 nmol) were separately dissolved in 200  $\mu$ L of PBS and then added to the activated CMC solution as two different reactions. The reactions proceeded at 4  $^{\circ}$ C overnight. The solutions were then twice precipitated in a saturated solution of ammonium sulfate, and the product was recovered by centrifugation. The pellets were reconstituted in PBS and followed by dialysis using Fast Spin Dialyzer and MWCO 300 kDa cellulose membrane (Nest Group) against pure PBS overnight with four changes of PBS.

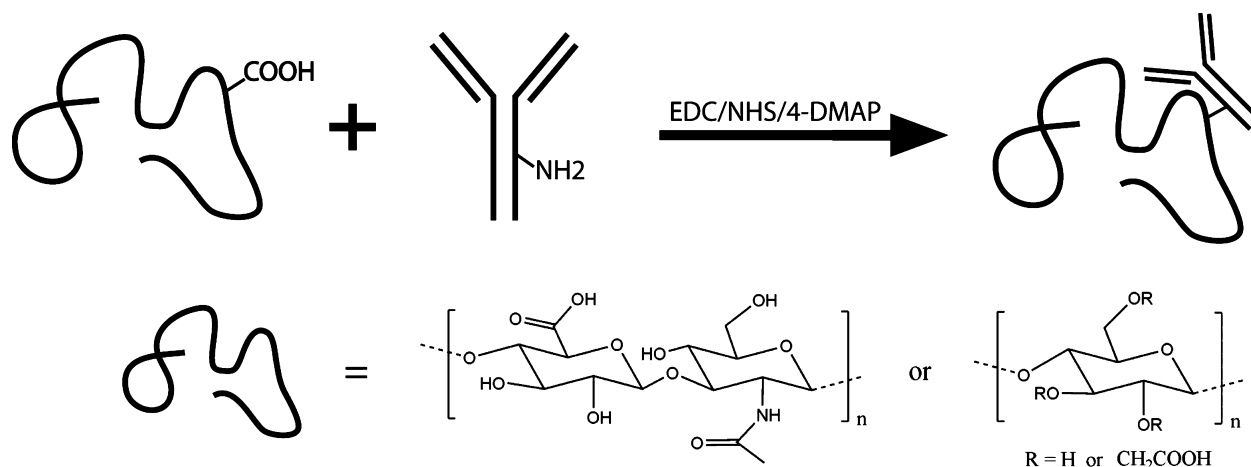
**2.3. Polyacrylamide Gel Electrophoresis.** A 10 mL solution of 4% acrylamide/bis-acrylamide solution in 0.5 $\times$

TBE buffer was prepared from 40% acrylamide/bis-acrylamide solution (Sigma, St. Louis, MO) and 10 $\times$  TBE buffer (Promega, Madison, WI). The solution was mixed on a stir plate for 10 min, and followed by adding 50  $\mu$ L of 10% (w/v) ammonium persulfate and 4  $\mu$ L of *N,N,N',N'*-tetramethylethylenediamine (Sigma, St. Louis, MO). The solution was well mixed and injected between glass plates (Bio-Rad, Hercules, CA). The gel set after 30–60 min. Then 5  $\mu$ L of each of the standards consisting of 1 mg/mL, 0.5 mg/mL, 0.25 mg/mL, 0.125 mg/mL, and 0.0625 mg/mL HA was loaded and the samples were loaded at two different concentrations using 1 $\times$  and 0.1 $\times$  stock solutions, and 125 V was used to electrophorese the gel for 5 h. Gels were stained in 0.5% (w/v) Alcian Blue (Sigma) with 3% (v/v) acetic acid for 45 min followed by destaining with 3% acetic acid overnight. Gel images were taken and quantitatively analyzed using Fujifilm LAS-3000 and MultiGauge image analysis software. CMC was quantified using the same procedure as that of HA with one condition modified. Since CMC was lower in molecular weight than HA, the PAGE was run for 3 h at constant voltage of 125 V.

**2.4. Fluorescence Immunosorbent Assay.** Immuno 96 MicroWell Plate (NUNC, Rochester, NY) was first incubated with 50  $\mu$ L of 1  $\mu$ g/mL of rabbit anti-rat IgG (Jackson ImmunoResearch, West Grove, PA) in PBS each well at 4  $^{\circ}$ C overnight. The solution was removed and the plate was washed three times with detergent followed by incubation at 37  $^{\circ}$ C for 1 h in 200  $\mu$ L of the blocking buffer, which contained 0.25% BSA, 0.05% Tween, and 1 mM EDTA in 1 $\times$  PBS. The plate was subsequently washed with PBS. Interleukin-1 antibody was dissolved in carbonate buffer, and standards were prepared using rat whole IgG (Jackson ImmunoResearch) in triplicate. Each solution was loaded at 50  $\mu$ L into a designated well followed by 1 h of incubation with shaking at room temperature. The solutions were discarded, and each well was washed in detergent three times with 10 min of incubation in between. Goat anti-rat IgG conjugated with Alexa 488 (Invitrogen, Carlsbad, CA) was diluted in carbonate buffer to the concentration of 2  $\mu$ g/mL, and loaded with 50  $\mu$ L into each well followed by 1 h incubation with shaking in the dark at room temperature. Wells were washed again three times with detergent for 10 min in between and the plates preserved with PBS. The plate was read and analyzed by SAFIRE microplate reader (Tecan, Mannedorf, Switzerland) with excitation at 488 nm and emission at 520 nm.

**2.5. Binding Affinity Measurements.** The Octet QK system (ForteBio Corp., Menlo Park, CA) was utilized to measure binding affinities of unmodified and conjugated mAb for their cytokines. The Octet measures the reflection coefficient as broadband visible light propagates to the end of a fiber optic. Changes in the refractive index at the fiber optic–solution interface result in a wavelength-dependent shift in the maximum of the reflection coefficient. Association and dissociation curves are fit to equations of the following form:

- (31) Homma, A.; Sato, H.; Okamachi, A.; Emura, T.; Ishizawa, T.; Kato, T.; Matsuura, T.; Sato, S.; Tamura, T.; Higuchi, Y.; Watanabe, T.; Kitamura, H.; Asanuma, K.; Yamazaki, T.; Ikemi, M.; Kitagawa, H.; Morikawa, T.; Ikeya, H.; Maeda, K.; Takahashi, K.; Nohmi, K.; Izutani, N.; Kanda, M.; Suzuki, R. Novel hyaluronic acid-methotrexate conjugates for osteoarthritis treatment. *Bioorg. Med. Chem.* **2009**, *17* (13), 4647–56.
- (32) Oh, E. J.; Park, K.; Choi, J. S.; Joo, C. K.; Hahn, S. K. Synthesis, characterization, and preliminary assessment of anti-Flt1 peptide-hyaluronate conjugate for the treatment of corneal neovascularization. *Biomaterials* **2009**, *30* (30), 6026–34.
- (33) Kuo, J. W.; Swann, D. A.; Prestwich, G. D. Chemical modification of hyaluronic acid by carbodiimides. *Bioconjugate Chem.* **1991**, *2* (4), 232–41.

**Scheme 1.** Preparation of Polysaccharide–Antibody Conjugates<sup>a</sup>

<sup>a</sup> Polysaccharides were partially activated at carboxylic acid sites followed by coupling reaction with pendant amines on the mAb (H<sub>2</sub>N-mAb). Carboxymethylcellulose (CMC) and hyaluronic acid (HA) were used as two representative polysaccharides.

$$R(t) = R_0 + \Delta R \{1 - \exp[-k_{\text{on}}(t - t_{\text{on}})]\} \quad (1)$$

$$R(t) = R_0 + \Delta R \exp[-k_{\text{off}}(t - t_{\text{off}})] \quad (2)$$

where  $R(t)$  is the reflection coefficient at time  $t$ ,  $R_0$  is the baseline value of the reflection coefficient,  $\Delta R$  is the total change in response,  $k_{\text{on}}$  is the association rate constant,  $t_{\text{on}}$  is the time at which the sensor is placed in solution containing the analyte,  $k_{\text{off}}$  is the dissociation rate constant, and  $t_{\text{off}}$  is the time at which the sensor is placed in pure buffer solution. The values for  $k_{\text{on}}$  and  $k_{\text{off}}$  are determined from curve fitting, and their ratio provides a measurement of  $K_D$ . Streptavidin sensor tips were hydrated in Kinetic Buffer (0.02% Tween 20, 150 mM NaCl, 1 mg/mL BSA, 10 mM phosphate buffered saline, and 0.05% sodium azide) supplied by ForteBio for at least 5 min before the experiment. All the samples were then diluted in Kinetic Buffer: mAb and polysaccharide–mAb were diluted to 10  $\mu\text{g/mL}$ . The experimental setup was performed in the following sequence: Kinetic Buffer 5 min (baseline), mAb or polysaccharide–mAb solution 10 min (loading), Kinetic Buffer 5 min (baseline), cytokine solution 30 min (association), and Kinetic Buffer 60 min (dissociation). The results were analyzed by the ForteBio analysis program that generated the best-fit binding isotherm and the association rate  $k_{\text{on}}$  and dissociation rate  $k_{\text{off}}$  were calculated from the isotherm.

**2.6. Imaging Cytometry.** THP-1 human acute monocytic leukemia cells were cultured at concentrations between 0.5 and  $7 \times 10^5$  cells/mL in RPMI 1640 (Cellgro, Manassas, VA), containing 10% FCS, L-glutamine, 100 U/mL penicillin, and 100  $\mu\text{g/mL}$  streptomycin, and maintained at 37 °C in 5% CO<sub>2</sub>. THP-1 cells were plated at 15,000 cells/well. Each well was treated with media containing 20 nM of PMA for 48 h at 37 °C followed by 24 h of recovery in fresh media before analysis.

Cells were stimulated according to each experimental condition for 30 min. The supernatants were gently aspirated and stimulated cells were fixed with 4% paraformaldehyde

in plates for 10 min. They were then subsequently washed once in PBS and permeabilized for 10 min with permeabilizing buffer. They were incubated in the presence of 1  $\mu\text{g/mL}$  anti-NF- $\kappa\text{B}$  antibodies for 1 h. Cells were treated with detergent for 10 min followed by 1 h incubation in the presence of 2  $\mu\text{g/mL}$  secondary antibodies and 1  $\mu\text{g/mL}$  solution of Hoechst 33342. Cells were then treated with detergent for 10 min, and 200  $\mu\text{L}$  of PBS was added to each well. Plates were covered and stored at 4 °C until analysis.

**2.7. Data Acquisition and Analysis.** The ArrayScan VTI imaging cytometer (Cellomics, Pittsburgh, PA) is an automated fluorescence microscope that acquires spatial information of the fluorescently labeled component in cells. The system scans a designated number of several fields in each individual well. Analysis of the images of each well was conducted according to a predefined algorithm. The system acquired images of the fields in each well until a predefined number of cells been identified and analyzed. The ArrayScan was equipped with emission and excitation filters for different fluorescent signals (Omega, Brattleboro, VT) emitted by Hoechst 33342, Alexa 488, and Alexa 680. Data were acquired and analyzed by ArrayScan Compartmental Analysis Bioapplication version 5.5.1.3 and HCS viewer (Cellomics). The Compartmental Analysis Bioapplication Software measures the average and total fluorescence intensity of specified subcellular regions, in this case the nucleus and cytosol. In our experiments, the software measured the average fluorescence intensity of NF- $\kappa\text{B}$  specific stain inside the nucleus. This value is subtracted from the mean fluorescent intensity of NF- $\kappa\text{B}$  in the cytosol to generate a mean value of translocated protein. That is used to subtract the average fluorescence intensity of NF- $\kappa\text{B}$  specific stain in specified donut ring around the nucleus. The difference demonstrated a measure of amount of NF- $\kappa\text{B}$  translocation, which was an indication of the level of cellular inflammatory response.

### 3. Discussion

**3.1. HA–mAb and CMC–mAb Composition.** Monoclonal IgG antibodies that were capable of neutralizing proinflammatory cytokines TNF- $\alpha$  and IL-1 $\beta$  were separately conjugated to HA and CMC using carbodiimide coupling chemistry, as shown in Scheme 1. Carboxylic acid groups on HA and CMC were first activated by sulfo-NHS through EDC-mediated chemical reaction. The antibodies were then introduced into the solutions of activated HA and CMC. In order to minimize possible cross-linking of polysaccharide through the formation of two or more amide bonds per antibody and also achieve one antibody per HA chain, the concentrations were kept low and the molar ratio of mAb to HA was less than one. First, HA was modified with the ratio of 21 carboxylate groups to 1 equiv of EDC and excess NHS. Assuming that the reactions go to completion, it would result in approximately 200 activated ester groups per HA chain. In the next step, mAb were introduced to the reaction with molar ratio of mAb to HA close to 1. Theoretically, this reaction scheme would produce conjugate product with mAb:HA molar ratio equal to 90%. In the CMC–mAb conjugate synthesis, the molar ratio was 20% to achieve a closer number of antibodies per unit volume of sample at similar polysaccharide mass fractions.

It was assumed that the primary amine groups on the antibodies reacted with NHS to form amide linkage, although theoretically this reaction will be equally efficient for amines in the Fab and Fc regions of the mAb. Binding affinity and cell assays served as preliminary tests of the resultant activities of the conjugates.

Following conjugation, samples were purified using ammonium sulfate precipitation followed by dialysis against PBS. In these experiments, dialysis was performed using a spinning dialysis chamber that improved the separation efficiency. The membrane had a 300 kDa MWCO to remove unconjugated mAb. Control experiments were performed in which polysaccharides and mAb were mixed in the absence of coupling reagents. Following dialysis, ELISA was performed to measure mAb concentration, which was found to be below the sensitivity limits of this technique ( $\sim 10$  ng/mL; data not shown). This suggests that our purification method was capable of removing mAb that was not conjugated to high molecular weight polysaccharide and that the binding affinity and cell assay results may be attributed to the polysaccharide–mAb conjugates.

In order to measure the composition of the conjugates, the concentrations of polysaccharide and mAb were measured separately. The method to measure the concentration of HA using nondenaturing PAGE was described previously by Sun et al.,<sup>21</sup> and the same 4% gel was applied to measure the concentration of CMC. A representative gel is shown in Figure 1A. It is difficult to determine whether any shifts in the bands occurred in the HA–mAb conjugates relative to the concentration standards based on unmodified HA. The CMC had an average molecular weight nearly five times that of the mAb, so any shifts could be small compared to the

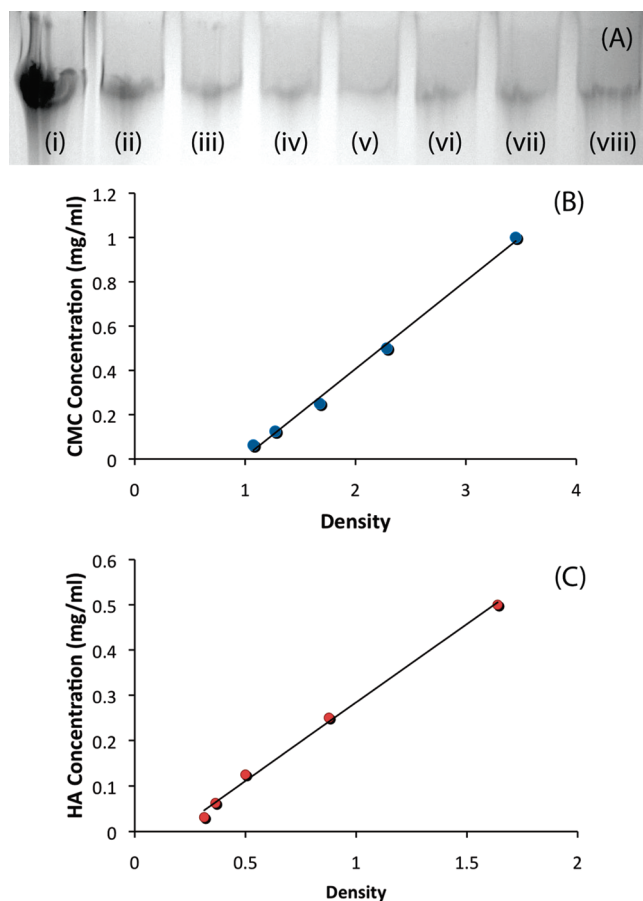


**Figure 1.** (A) Nondenaturing polyacrylamide gels, stained with Alcian blue, showing the results from analyzing HA samples with varying concentration with and without conjugated mAb: (i) 0.5 mg/mL HA, (ii) 0.25 mg/mL HA, (iii) 0.13 mg/mL HA, (iv) 0.06 mg/mL HA, (v) 0.03 mg/mL HA, (vi)  $0.1\times$  HA–anti-IL1 $\beta$  mAb, (vii)  $0.1\times$  HA–anti-TNF- $\alpha$  mAb, (viii)  $0.1\times$  HA + mAb. (B) CMC concentration calibration curve fit to the equation  $y = 0.0398x - 0.0388$ ,  $R^2 = 0.9965$ , (C) HA concentration calibration curve fit to the equation  $y = 0.0346x - 0.0062$ ,  $R^2 = 0.9964$ .

intrinsic breadth of the CMC bands. The integrated intensities of the bands were correlated with the serially diluted CMC standards to generate a calibration curve, shown in Figure 1B. Due to the high molecular weight of CMC, the gel was saturated at CMC concentrations of 2 mg/mL and excessive spreading of the bands was observed. In order to accurately estimate the concentration of CMC in the conjugate, highest concentration was determined to be 1 mg/mL, and all the samples were diluted 1:10 to fit in the range of the calibration curve. Results are tabulated in Table 1.

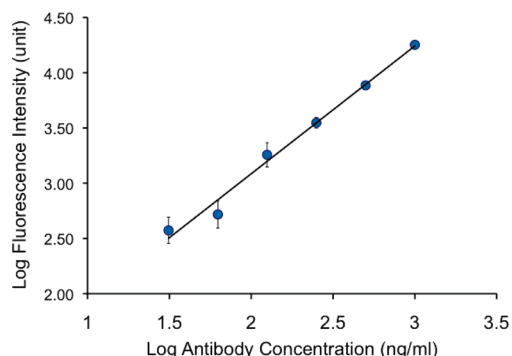
Sandwich fluorescence immunosorbent assays were utilized to quantitatively determine the concentration of monoclonal antibody in the conjugates. A calibration curve was generated using rat whole IgG, and the results are shown in Figure 2. The concentrations of the antibodies in the different conjugate systems are shown in Table 1, as well as the ratios of mAb to polysaccharide.



**Table 1.** Summary of Compositions Determined from PAGE and Fluorescence Immunosorbent Assays<sup>a</sup>

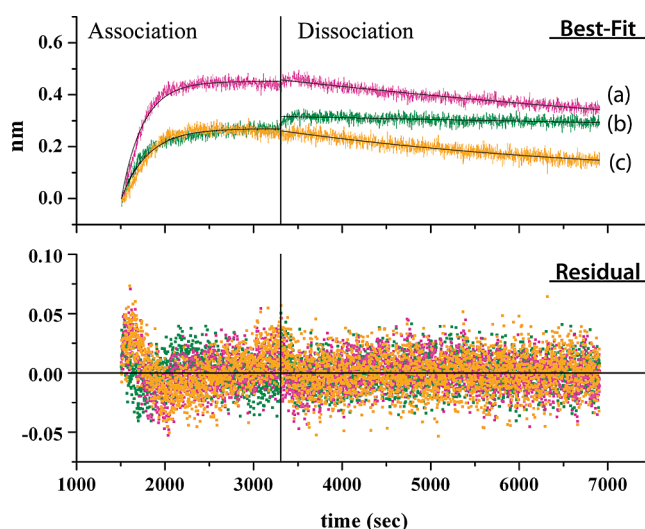
	concn ( $\mu$ M)		mAb:polysaccharide (mol %)
	polysaccharide	antibody	
HA–anti-IL-1 $\beta$	0.77	0.48 $\pm$ 0.03	62 $\pm$ 3
HA–anti-TNF- $\alpha$	1.21	0.44 $\pm$ 0.06	36 $\pm$ 5
CMC–anti-IL-1 $\beta$	7.37	0.53 $\pm$ 0.04	7 $\pm$ 1
CMC–anti-TNF- $\alpha$	9.20	0.59 $\pm$ 0.09	6 $\pm$ 1

<sup>a</sup> Separate measurements of polysaccharide and antibody concentrations provide the basis for determining the degree of functionalization in polysaccharide–mAb conjugates.

**Figure 2.** Calibration curve from fluorescence immunosorbent assay of mAb concentration in polysaccharide–mAb conjugates. Data were fit to  $y = 1.1572x + 0.771$  ( $R^2 = 0.9878$ ).

The experimental results are summarized in Table 1. Defining the reaction efficiency as the ratio of the experimental and theoretical yields (90% for HA and 20% for CMC), the HA–anti-IL-1 $\beta$  reaction had an efficiency of 69% and the HA–anti-TNF- $\alpha$  was 40% while CMC–anti-IL-1 $\beta$  was 35% and CMC–anti-TNF- $\alpha$  was 30%. It is not clear why the HA–anti-IL-1 $\beta$  conjugation reaction appeared to be significantly more efficient than the other reactions. However, for the purposes of measuring binding affinities, the conjugates should coat the sensor surface equally well, as discussed in section 3.2.

**3.2. Cytokine Binding Affinity of HA–mAb and CMC–mAb Conjugates.** The binding constants of the four different conjugates of polysaccharide and mAb were measured and compared to the nonconjugated anti-IL-1 $\beta$  and anti-TNF- $\alpha$  mAb. All mAb were biotinylated to bind strongly with streptavidin-functionalized sensor tips. The rise in signal, shown in Figure 3, demonstrated the change in refractive index at the sensor–solution interface, indicating that the cytokines were interacting with the sensor surface coated with antibodies or conjugates via the mAb portion. After the signal reached saturation, the sensors were immersed in buffer solution to measure the dissociation of the cytokines from sensor surface. The association and dissociation curve were fit by eqs 1 and 2, respectively, to generate isotherms and obtain the corresponding binding constants. The standard deviations of the binding constants were calculated based on three separate measurements. Some baseline drift, attributed to instrument variability, was

**Figure 3.** Binding affinity analysis using Fortebio Octet system. (Top) Association, dissociation curve, and best-fit isotherms of different conditions: (a) anti-IL-1 $\beta$  mAb, (b) HA–anti-IL-1 $\beta$  mAb conjugate, (c) CMC–anti-IL-1 $\beta$  mAb conjugate. (Bottom) Plot of the residuals from the best-fit curve.**Table 2.** Summary of Measured Kinetics Constants Describing Interactions between mAb and Polysaccharide–mAb Conjugates with the Cytokines and the Calculated Equilibrium Binding Constants

	$k_{on}$ [ $10^5$ 1/(M s)]	$k_{off}$ ( $10^{-5}$ 1/s)	$K_D$ (pM)
anti-IL-1 $\beta$ mAb	6.55 $\pm$ 0.38	7.91 $\pm$ 1.68	118.0 $\pm$ 19.5
HA–anti-IL-1 $\beta$	6.25 $\pm$ 0.23	2.51 $\pm$ 0.32	40.1 $\pm$ 4.8
CMC–anti-IL-1 $\beta$	5.59 $\pm$ 0.60	24.44 $\pm$ 7.76	412.2 $\pm$ 1.3
anti-TNF- $\alpha$ mAb	6.45 $\pm$ 0.15	7.56 $\pm$ 0.47	117.2 $\pm$ 7.3
HA–anti-TNF- $\alpha$	13.60 $\pm$ 1.08	16.66 $\pm$ 0.92	123.0 $\pm$ 10.0
CMC–anti-TNF- $\alpha$	9.87 $\pm$ 0.61	14.16 $\pm$ 1.54	137.4 $\pm$ 20.0

observed during the lengthy dissociation experiments, which was corrected using a baseline subtraction. Therefore, both association and dissociation isotherms were corrected with corresponding subtractions to obtain reported results.

The results from affinity binding experiment are shown in Table 2. The  $K_D$  for both anti-IL-1 $\beta$  was measured to be 118.0  $\pm$  19.5 pM while that for HA–(anti-IL-1 $\beta$ ) was 40.13  $\pm$  4.79 pM and CMC–(anti-IL-1 $\beta$ ) was 412.2  $\pm$  1.30 pM. The association kinetics were essentially identical, with  $k_{on}$  values of  $(6.55 \pm 0.38) \times 10^5$ /(M s) for nonconjugated anti-IL-1 $\beta$ ,  $(6.25 \pm 0.23) \times 10^5$ /(M s) for HA–(anti-IL-1 $\beta$ ), and  $(5.59 \pm 0.60) \times 10^5$ /(M s) for CMC–(anti-IL-1 $\beta$ ). The main factor contributing to differences in  $K_D$  for the conjugates compared to the nonconjugated mAb appeared in the dissociation kinetics: IL-1 $\beta$  dissociated three times more slowly from the HA–(anti-IL-1 $\beta$ ) but three times faster from CMC–(anti-IL-1 $\beta$ ). This suggests that neither HA nor CMC interferes with the formation of the antigen–antibody complex, but HA appeared to stabilize this complex while CMC appeared to destabilize it. The exact mechanisms for these synergistic interactions are not clear, but the conjuga-

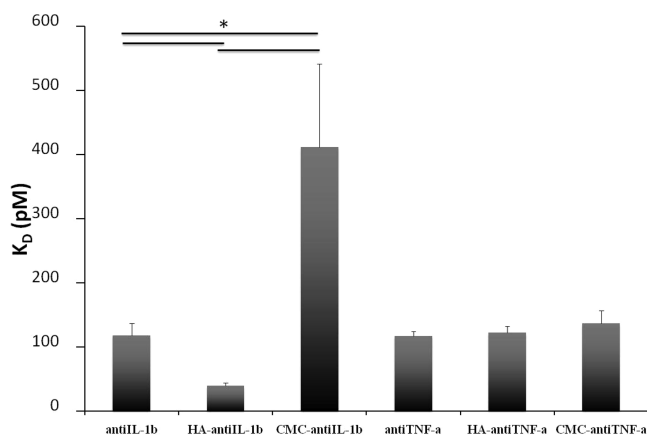


**Figure 4.** Binding constants ( $K_D$ ) measured and calculated using ForteBio Octet system. The results are shown as the average of the five separated measurements of each condition, and the error bars are shown as the standard deviation. (\*)  $p < 0.001$ .

tion of high molecular weight polysaccharides to anti-IL-1 $\beta$  can clearly influence the binding kinetics. Further experiments that probe conformation changes in the polysaccharide as a function of antigen binding may illuminate the effects observed.<sup>34</sup> However, in both constructs, IL-1 $\beta$  binding was still observed.

Nonconjugated anti-TNF- $\alpha$  was measured to have an equilibrium binding constant of  $117.2 \pm 7.34$  pM, also consistent with manufacturer's specifications. Both the HA-(anti-TNF- $\alpha$ ) and CMC-(anti-TNF- $\alpha$ ) conjugates had similar values of  $K_D$ :  $123.0 \pm 10.0$  pM and  $137.4 \pm 20.0$  pM, respectively. However, in both HA and CMC, the rate constants  $k_{on}$  and  $k_{off}$  were approximately two times slower, leaving the ratio of  $k_{off}$  to  $k_{on}$  similar but suggesting that adsorption and desorption of TNF- $\alpha$  to the constructs were slightly inhibited. TNF- $\alpha$  is a trimeric protein with a molecular weight that is three times greater than that of IL-1 $\beta$ , which may contribute to the differences in kinetics between conjugated and nonconjugated mAb. In binding anti-TNF- $\alpha$ , though, both polysaccharide conjugates appear to have good binding affinity. The results are summarized in Figure 4 and Table 2 for both anti-IL-1 $\beta$  and anti-TNF- $\alpha$  constructs.

**3.3. In Vitro Cytokine Neutralization by HA-mAb and CMC-mAb Conjugates.** In order to validate the biological activities of these conjugates, THP-1 human acute monocytic leukemia cells were differentiated into macrophages and exposed to solutions containing IL-1 $\beta$  or TNF- $\alpha$  with or without polysaccharide-mAb conjugates. Measuring the translocation of cytosolic NF- $\kappa$ B into the nucleus using

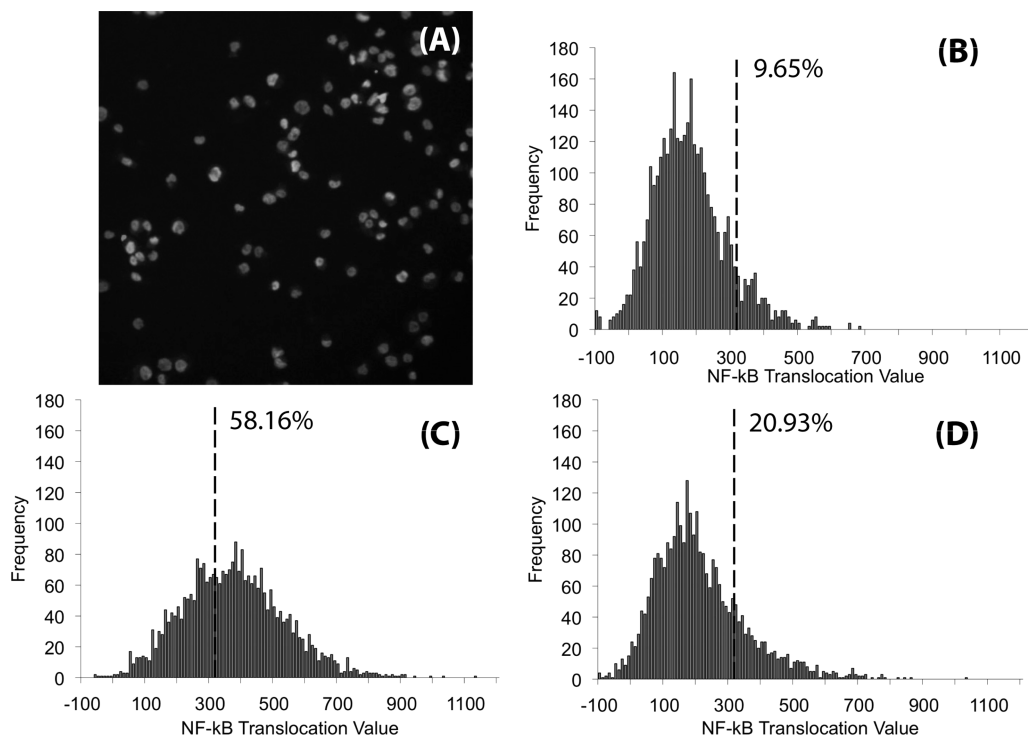


**Figure 5.** Imaging cytometry result of PMA-differentiated THP-1 macrophages stained with p65 subunit of nuclear factor-kappa B (NF- $\kappa$ B) and nucleus after stimulated by various different conditions. (A) Representative imaging cytometry image of THP-1 macrophages treated with 100 ng/mL of IL-1 $\beta$ . The nuclei appear as bright spots surrounded by bright rings, which represents the stained cytosolic NF- $\kappa$ B. (B–D) Histogram representation of the NF- $\kappa$ B translocation value of THP-1 macrophages treated with (B) culture media, (C) 100 ng/mL IL-1 $\beta$ , and (D) CMC-anti-IL-1 $\beta$  + 100 ng/mL IL-1 $\beta$ . A dashed line represents the 90th percentile of the unstimulated THP-1 macrophage population, and this translocation value of 320 was used as a threshold to identify responsive THP-1 cells in the stimulated populations. The number beside the dashed line in each histogram is the fraction of stimulated cells determined by the threshold.



imaging cytometry provides a method to quantify incipient inflammatory responses,<sup>35</sup> and images used for analysis are shown in Figure 5A. The compartment analysis protocol quantitatively measured and compared the amount of NF- $\kappa$ B stained in the nucleus and cytoplasm. The difference of the amounts of NF- $\kappa$ B measured in these two compartments was used as an indicator of the level of inflammatory stimuli. Increases in the translocation value are expected following exposure to proinflammatory cytokines, and lower levels should be observed if cytokines are neutralized by mAb in solution.

Following methods described elsewhere,<sup>36</sup> cells were classified as stimulated or unstimulated with an arbitrary threshold of the 90th percentile of the NF- $\kappa$ B translocation value in the negative control samples. Representative histograms are shown in Figure 5B–D. In Figure 5B is shown the histogram of translocation values for unstimulated cells, with the most probable value of 130 and the 90th percentile at 320. In cultures stimulated with IL-1 $\beta$ , 58% of the cells had translocation values above 320, as shown in Figure 5C, while cultures with IL-1 $\beta$  and CMC–(anti-IL-1 $\beta$ ) had 21% of the cells with translocation values above threshold. This suggests that CMC–(anti-IL-1 $\beta$ ) is effective at reducing the signaling of IL-1 $\beta$  in solution.

The results of histogram analyses across the different conditions are shown in Figure 6. When stimulated with LPS,  $53.3 \pm 7.7\%$  of cells had translocation values above threshold while  $58.2 \pm 5.6\%$  of those stimulated with IL-1 $\beta$  were above threshold and  $27.2 \pm 5.2\%$  when stimulated with TNF- $\alpha$ . Treatment with solutions containing IL-1 $\beta$ /anti-IL-1 $\beta$  and TNF- $\alpha$ /anti-TNF- $\alpha$  resulted in translocation values of  $16.7 \pm 5.3\%$  and  $14.4 \pm 6.4\%$ , respectively. This indicates that mAb are binding the cytokines and preventing most, but not all, NF- $\kappa$ B activation from occurring. For all compositions of CMC–mAb and HA–mAb conjugates, similar ranges of the translocation values were observed for neutralizing the effects of IL-1 $\beta$  or TNF- $\alpha$ , which indicates that the polysaccharide constructs have comparable cytokine-neutralizing activities as unmodified mAb.

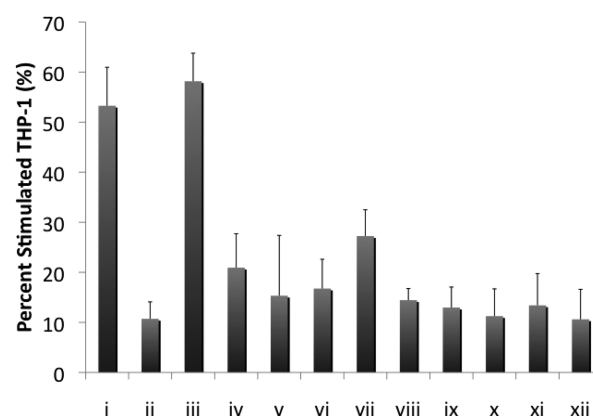


**Figure 6.** Fraction of the THP-1 cells with translocation values above the threshold defined as the 90th percentile in the unstimulated control group: (i) 100 ng/mL LPS, (ii) culture medium, (iii) IL-1 $\beta$ , (iv) 0.1 wt % CMC–anti-IL-1 $\beta$  + 100 ng/mL IL-1 $\beta$ , (v) 0.1 wt % HA–anti-IL-1 $\beta$  + 100 ng/mL IL-1 $\beta$ , (vi) 100  $\mu$ g/mL anti-IL-1 $\beta$  + 100 ng/mL IL-1 $\beta$ , (vii) 100 ng/mL TNF- $\alpha$ , (viii) 0.1 wt % CMC–anti-TNF- $\alpha$  + 100 ng/mL TNF- $\alpha$ , (ix) 0.1 wt % HA–anti-TNF- $\alpha$  + 100 ng/mL TNF- $\alpha$ , (x) 100  $\mu$ g/mL anti-TNF- $\alpha$  mAb + 100 ng/mL TNF- $\alpha$ , (xi) 1 mg/mL CMC, and (xii) 1 mg/mL HA. Error bars represent the standard deviation of four separate samples.

#### 4. Conclusions

Conjugation of mAb against the proinflammatory cytokines IL-1 $\beta$  or TNF- $\alpha$  to high molecular weight HA or CMC resulted in constructs that retained their cytokine binding affinities, although differences were observed in the dissociation kinetics suggesting that some antibody constructs have enhanced affinities while others were weakened through conjugation. Cell assays of the neutralization of cytokine signaling by these constructs confirmed their cytokine-binding functions in dilute solution.

**Acknowledgment.** Financial support was provided from U.S. Army DAMD 17-02-1-0717 (N.R.W.), Department of Defense W81XWH-08-2-0032 (N.R.W.), and NIH R43GM085897 (N.R.W.). N.R.W. also acknowledges support from a 3M Non-Tenured Faculty Grant. This report was funded, in part, by 1 P01 CA 101944-01A2 (M.T.L.) Integrating NK and DC into Cancer Therapy and under a special grant initiative on behalf of Jonathan Gray from The Sanford C. Bernstein and Company, LLC. The Clinical and Translational Research Program (Reis, Steven; 1U54RR-023506-01) Catalyst Program for support of LTS is also gratefully acknowledged. One author (N.R.W.) has formed a company to commercialize aspects of this research and acknowledges a potential conflict of interest.

MP100150Z

- (34) Liu, Y.; Meng, S.; Mu, L.; Jin, G.; Zhong, W.; Kong, J. Novel renewable immunosensors based on temperature-sensitive PNIPAAm bioconjugates. *Biosens. Bioelectron.* **2008**, *24* (4), 710–5.
- (35) Vakkila, J.; DeMarco, R. A.; Lotze, M. T. Imaging analysis of STAT1 and NF-kappaB translocation in dendritic cells at the single cell level. *J. Immunol. Methods* **2004**, *294* (1–2), 123–34.
- (36) Moore, D. L.; Blackmore, M. G.; Hu, Y.; Kaestner, K. H.; Bixby, J. L.; Lemmon, V. P.; Goldberg, J. L. KLF family members regulate intrinsic axon regeneration ability. *Science* **2009**, *326* (5950), 298–301.